https://doi.org/10.5194/egusphere-2023-340
Preprint. Discussion started: 7 March 2023

The impact of model resolution on the Southern Hemisphere in CCSM4 idealized climate simulations

Houraa Daher[1], Ben P. Kirtman[1]

[1]Rosenstiel School for Marine, Atmospheric, and Earth Science, University of Miami, Miami, FL, USA

Correspondence to: Houraa Daher (hdaher@earth.miami.edu)

Abstract. Ocean model resolution plays a large role in accurately simulating the Southern Hemisphere circulation in both the ocean and atmosphere. Resolving the ocean mesoscale field is important as it has been shown to have a significant impact on the large-scale climate in eddy rich regions (i.e., western boundary currents, the Antarctic Circumpolar Current) which also are regions of large CO_2 absorption. The presence of ocean mesoscale features can affect sea surface temperatures, the strength and location of the storm tracks, and many other air-sea processes. Additionally, with an improvement in resolution, the eddy kinetic energy in the ocean can be expected to change considerably. The significance model resolution has on the Southern Hemisphere is examined using Community Climate System Model, version 4 ocean eddy-parameterizing and eddy-resolving simulations. The CO_2 concentrations and ozone levels are specified independently to better understand how the mesoscale field responds to extreme changes in the external forcing and the resulting climate impacts. Overall, in the eddy-parameterizing simulations, the ozone forcing is found to be more important than the changes in CO_2 concentrations for the zonal mean atmospheric temperature, zonal mean zonal wind, sea surface temperature, sea surface height, eddy kinetic energy, zonal mean ocean temperature, convective precipitation, and surface temperature. In the case of the eddy-resolving simulations, however, the CO_2 concentrations are found to be more dominant, especially in eddy-rich regions.

1 Introduction

Ocean model resolution within global climate models has been shown to be of great importance when simulating the Southern Hemisphere climate. With an increase in model resolution, ocean mesoscale features are better resolved and play a large role in improving the accuracy of the large-scale climate within these models. These mesoscale features, such as ocean eddies, have a significant impact on the ocean circulation, atmosphere, and air-sea interactions (Hewitt et al., 2016, Small et al., 2008, 2019, 2020, Chang et al., 2020), especially in eddy-rich regions like western boundary currents and their extensions (Small et al., 2008; Bryan et al., 2010; Kelly et al., 2010; Ma et al., 2016; Putrasahan et al., 2013, 2017). In these regions, the mesoscale activity in the ocean drives the atmosphere with turbulent heat fluxes out of the ocean and into the atmospheric boundary layer (Bryan et al., 2010). Global climate models that use low-resolution ocean components are unable to capture these physical processes and therefore miss a large part of the climate picture. This study analyzes the importance of the ocean mesoscale field in the Southern Hemisphere using Community Climate System Model, version 4 (CCSM4) ocean eddy-resolving and eddy-parameterizing simulations.

https://doi.org/10.5194/egusphere-2023-340
Preprint. Discussion started: 7 March 2023

The significance of ocean model resolution on the Southern Hemisphere in CCSM4 has been demonstrated in previous studies. Bryan et al., (2010) find that there is a positive correlation between sea surface temperature and surface wind stress when the ocean component is eddy-resolving. With an increase in model resolution, there is a stronger forcing of the atmosphere by the sea surface temperature variability in the extra-tropics that is found to be weak in the low-resolution model and regions of high mesoscale activity like western boundary currents are found to have a warmer sea surface temperature (Kirtman et al., 2012). Around Antarctica however, the ocean warming response is found to be weaker with the presence of eddies in the model (Bitz and Polvani, 2012; Bilgen and Kirtman, 2020). Additionally, a more accurate Agulhas Current, retroflection, and leakage estimate is resolved using high-resolution eddy-resolving simulations (McClean et al., 2011; Kirtman et al., 2012; Putrasahan et al., 2015; Cheng et al, 2016).

Resolving the mesoscale features in these global climate models is not only important for understanding the physical processes, but also for understanding the large-scale climate. Ocean eddies play a large role in the uptake of the anthropogenic CO_2 (Gnanadeskikan et al., 2015) and with 40% of the oceanic uptake of CO_2 occurring south of 40°S (Sallée et al., 2012). Additionally, resolving western boundary currents and their extensions has been shown to be as important with these regions being hotspots of ocean warming, especially over the last few decades where they have been warming at a rate 3-4 times the global average (Wu et al., 2012; Oliver and Holbrook, 2014; Goyal et al., 2021). With the anthropogenic climate change in the Southern Hemisphere being primarily driven by CO_2 concentrations and stratospheric ozone levels, the mesoscale field plays a significant role in changes to these atmospheric forces and therefore influences the Southern Hemisphere climate. How the mesoscale field responds to changes in CO_2 concentrations and ozone levels is then examined in this study.

Bitz and Polvani (2012) investigate the Antarctic climate response to stratospheric ozone depletion in CCSM4 and find that there is warming in the ocean down to 1000 m and reduced sea ice extent. They find that with the presence of ocean eddies, the warming is weaker, but the total loss of sea ice area is comparable between the eddy-resolving and eddy-parameterizing simulations. The weaker warming response in the presence of eddies is a process known as eddy compensation, in which the mesoscale eddies oppose the wind-driven upwelling that is often seen with increased CO_2 concentrations and stratospheric ozone depletion and therefore prevent long term warming (Doddridge et al., 2019). Using observations and climate models, Swart et al. (2019) find that the Southern Ocean warming and freshening is driven primarily by an increase in anthropogenic greenhouse gases and that the effect of the stratospheric ozone depletion is secondary. Using a unique coupled climate model with enhanced ocean resolution, Ivanciu et al. (2022) investigate the impact of increased greenhouse gases and ozone recovery on the Southern Hemisphere and find the westerly winds weaken and shift equatorward due to ozone recovery resulting in a decrease in transport of the Antarctic Circumpolar Current (ACC) and in Agulhas leakage. They also find warming in the upper ocean associated with increased greenhouse gases that overwhelms the ozone recovery signal.

https://doi.org/10.5194/egusphere-2023-340
Preprint. Discussion started: 7 March 2023

The impact of model resolution on the Southern Hemisphere in CCSM4 is studied using ocean eddy-parameterizing and eddy-resolving simulations. Past CO_2 concentrations and stratospheric ozone levels are specified independently to simulate idealized climate states to investigate what role the presence of ocean eddies play in the Southern Hemisphere large-scale ocean circulation and air-sea interactions. This paper compares the individual responses of low-resolution eddy-parameterizing simulations against high-resolution eddy-resolving simulations when the external forcing is idealized to include an increase in CO_2 concentrations and stratospheric ozone levels from the mid-twentieth century. The results presented here are not intended to be interpreted as projections or predictions. The intent is to diagnose how the response to large changes in CO_2 and ozone concentrations differ in ocean eddy parameterized vs. eddy permitting global coupled simulations.

2 Methods

This study analyzes model output from NCAR's CCSM4 coupled-climate model (Gent et al., 2011). The ocean and atmosphere models used in CCSM4 are Parallel Ocean Program, version 2 (POP2) and Community Atmosphere Model, version 4 (CAM4), respectively. POP2 has 60 vertical layers with 10 m layer thickness in the first 100 m and slowly increasing to 250 m at 6000 m depth. CAM4 has 26 vertical layers in the atmosphere. The stratospheric and tropospheric ozone is calculated semi-offline using the interactive chemistry in CAM-Chem, the chemistry version of CAM (Lamarque et al., 2010, 2011, 2012; Meehl et al., 2012; Eyring et al., 2013).

Model output from six simulations is used, a combination of two model resolutions and three idealized experiments (Table 1). The eddy-parameterizing simulations are low-resolution with 1° in the ocean and atmosphere and the eddy-resolving simulations are high-resolution with 1/10° in the ocean and 1/2° in the atmosphere. The first idealized experiment (named LRC07 for the low-resolution simulation, and HRC07 for the high-resolution simulation) is the 20th century climate change simulation with corresponding CO_2 levels applied (Kirtman et al., 2012, Fig. 1a, blue line). The ozone levels in this experiment are kept constant at year 2000 levels, a time representative of a depleted ozone (Fig 1b, red line). There are 100 years of data available for LRC07 (1910-2010) and 70 years of data available in HRC07 (1940-2009). The LRC07 and HRC07 simulations are interpreted as idealized experiments examining how changes in CO_2 concentrations affect Southern Hemisphere climate with fixed (depleted) ozone concentrations. We assert here that this approach is useful in terms of separating the effects of CO_2 changes vs. ozone changes. The second idealized experiment (LRC08 and HRC08) is the control experiment with the ozone levels also kept constant at year 2000 levels. The CO_2 forcing however, differs from the previous experiment in that it is also kept constant at year 2000 levels (379 ppm, Fig. 1a, red line). Like LRC07 and HRC07, 100 years of data is available for LRC08 and 70 years of data is available for HRC08. LRC08 and HRC08 are used as the control experiment as the CO_2 concentrations and ozone levels are both kept constant unlike the other experiments. Any differences between the control experiment and the other experiments can therefore be attributed to changes in the forcing parameters. The last idealized experiment (LRC20 and HRC20) uses constant year 2000 CO_2 forcing (Fig 1a, red line) like the control experiment, but sets the ozone to year 1955 levels, a time representative of a healthier ozone (Fig 1b, blue line). LRC20 has 100

https://doi.org/10.5194/egusphere-2023-340
Preprint. Discussion started: 7 March 2023

years of data, however, HRC20 only has 18 years of data available as the mean climatic effects become clear in a relatively short period of time. Month mean outputs are considered in this study.

The first objective in comparing these simulations is to identify any differences between the eddy-parameterizing and eddy-resolving experiments with specific attention to Southern Hemisphere climate. The second objective is to examine what role the difference in model resolution plays in the idealized experiments and how the presence of a more robustly represented mesoscale field affects the response to changes in atmospheric forcing, specifically changes in the atmospheric CO_2 and ozone levels. To examine the Southern Hemisphere response to changes in CO_2 (while holding the ozone levels constant), a difference between the time averaged mean of the high concentrations warming experiment (LRC08 and HRC08) and time averaged mean of the low concentrations cooling experiment (LRC07 and HRC07) is taken. These differences are referred to as LRC_{CO2} and HRC_{CO2}. The same can be done to determine the Southern Hemisphere response to changes in the ozone (while holding the CO_2 levels constant) by taking a difference between the time averaged mean of the healthier ozone experiment (LRC20 and HRC20) and the time averaged mean of the depleted ozone experiment (LRC08 and HRC08). These differences are referred to as LRC_{O3} and HRC_{O3}. Because the radiative forcing associated with the changes in CO_2 and O_3 are different, the results are normalized by the global mean temperature change to put them on equal footing. LRC_{CO2}, HRC_{CO2}, LRC_{O3}, and HRC_{O3} are divided by the difference in the global mean surface air temperature (2 m temperature) for their respective experiments. The normalized quantities are interpreted as the response per degree global mean temperature change. This normalization allows for quantitative comparisons of the CO_2 vs. O_3 response. This approach of normalizing by global mean temperature is seen in previous climate studies (Holland and Bitz, 2003; Vecchi and Soden, 2007; Soden and Vecchi, 2011; Zhao et al., 2017; Lin et al., 2018; Hahn et al., 2021; Rantanen et al., 2022). Lastly, to find the net change and whether the CO_2 or ozone forcing is more dominant, a sum of the CO_2 and ozone differences is taken.

For the GHG forcing, change per degree of warming:

$$LRC_{CO2}/HRC_{CO2} = \frac{LRC08/HRC08 - LRC07/HRC07}{|\overline{TS}_{LRC08/HRC08} - \overline{TS}_{LRC07/HRC07}|}$$

For the O_3 forcing, changer per degree of cooling:

$$LRC_{O3}/HRC_{O3} = \frac{LRC20/HRC20 - LRC08/HRC08}{|\overline{TS}_{LRC20/HRC20} - \overline{TS}_{LRC08/HRC08}|}$$

The sum of these normalized maps is then used to get the net change:

$$LRC_{Total}/HRC_{Total} = LRC_{CO2}/HRC_{CO2} + LRC_{O3}/HRC_{O3}$$

3 Results

The following figures (Figs. 2-9) show the mean differences between the ocean eddy-parameterizing and eddy-resolving simulations as well as the differences between the increased CO_2 concentrations and ozone of the past. The

https://doi.org/10.5194/egusphere-2023-340
Preprint. Discussion started: 7 March 2023

first row shows the results from the eddy-parameterizing experiments (LRC) and the second row shows the results from the eddy-resolving experiments (HRC). The first, second, and third column show results from LRC_{CO2}/HRC_{CO2}, LRC_{O3}/HRC_{O3}, and LRC_{Total}/HRC_{Total}, respectively.

3.1 Zonal mean atmospheric temperature

Because the atmospheric resolution also changes in addition to the ocean resolution, the atmospheric variables are investigated first to determine whether changes seen in the ocean can be potentially attributed to the resolution change in the atmosphere. The next two figures (Fig. 2 and Fig. 3) examine the response to the zonal mean atmospheric temperature and zonal mean zonal wind. The zonal mean temperature throughout the atmosphere is calculated at each latitude (Fig. 2). In LRC_{CO2} (Fig. 2a), there is warming seen throughout the Southern Hemisphere except in the lower stratosphere poleward of 50°S, where the ozone is depleted. The strongest changes in temperature are seen at 100 mb with an increase (decrease) of over two-degrees equatorward (poleward) of 50°S. The high-resolution equivalent, HRC_{CO2} (Fig. 2d), shows a similar response as LRC_{CO2} with cooling in the lower stratosphere, but this cooling extends beyond the high-latitudes to the equator in the top 100 mb. There is also slight cooling seen at the surface in the high-latitudes that is not present in the low-resolution simulation.

The LRC_{O3} (Fig. 2b) map shows an opposite and more intense pattern to LRC_{CO2}, with a stronger warming seen in the lower stratosphere poleward of 50°S. Warming of much greater than two-degrees is seen when the ozone levels were representative of the past. A healthy ozone above Antarctica means most of the incoming solar radiation will be absorbed by the lower stratosphere at the high-latitudes and there will be less warming throughout the atmosphere. HRC_{O3} (Fig. 2e), also shows warming in the lower stratosphere at the high-latitudes but it is not as strong as in LRC_{O3}. There is, however, strong cooling of more than two-degrees seen equatorward of 55°S between 200 and 600 mb that is not present in LRC_{O3}.

The intense warming seen in LRC_{O3} (Fig. 2b) is also present in LRC_{Total} (Fig. 2c), suggesting that the ozone forcing dominates in the lower stratosphere. The rest of the atmosphere has little to zero temperature change with the two responses largely cancelling each other out. The overall net change seen in HRC_{Total} (Fig. 2f) is slightly different from LRC_{Total} as there is only a small region of the lower stratosphere warming at the high latitudes and cooling associated everywhere else. The upper 100 mb looks to be controlled by the increase in CO_2 concentrations whereas the rest of the Southern Hemisphere shows a response similar to the 1955 ozone simulation. Overall, the biggest change observed with an increase in atmospheric resolution is the magnitude of change, but the pattern between the two remains consistent with the ozone forcing being more important than the CO_2 concentrations, particularly for the eddy-resolving simulations.

3.2 Zonal mean zonal wind

https://doi.org/10.5194/egusphere-2023-340
Preprint. Discussion started: 7 March 2023

The same calculation for the temperature is done for the zonal wind (Fig. 3) and the patterns seen in the LRC simulations (Fig. 3a-c) are all relatively weak compared to the HRC simulations (Fig. 3d-f). In LRC_{CO2}, there is an increase in the zonal wind found in the upper 200 mb at the mid-latitudes and a slight increase in the westerlies and towards the equator. There is a decrease in zonal wind seen at the trade wind latitudes. The pattern seen in HRC_{CO2} (Fig. 3d) is similar to LRC_{CO2} but much stronger. There is a strong increase in the westerlies and upper troposphere equatorward of 55°S.

Similar to what was observed with the zonal mean temperature (Fig. 2), the opposite pattern to LRC_{CO2} is shown for the LRC_{O3} (Fig. 3b) simulation, with a slight decrease in the westerlies and a stronger decrease observed in the upper 200 mb. For HRC_{O3} (Fig. 3e), however, the signal is much more amplified throughout the atmosphere and there is a strong weakening of the westerly jet and upper troposphere.

LRC_{Total} (Fig. 3c) shows very little change with the exception of the upper 100 mb resembling the LRC_{O3} simulation. HRC_{Total} (Fig. 3f) shows a different response and that equatorward of 50°S the increase in CO_2 concentrations plays a larger role and poleward of 50°S, the ozone is more important. It is also clear in the low-resolution simulations, that there is no poleward or equatorward shift of the westerlies, whereas the high-resolution simulations show an equatorward shift and weakening of the westerly jet.

While there are slight differences in the methods of showing the results, the zonal mean temperature and zonal mean zonal wind in this study (Fig. 2 and Fig.3) are compared with those in Fig. 1 from Polvani et al. (2011), who use an atmospheric model (CAM3, 2.8° × 2.8° horizontal resolution) and are found to be in good agreement. With an increase in concentrations, Polvani et al. (2011) find a decrease in the temperature at the high-latitudes in the lower stratosphere that extends to the equator in the upper 100 mb and an increase in temperature everywhere else in the Southern Hemisphere, a result consistent with HRC_{CO2} (Fig. 2d). In their ozone recovery simulation, they find intense warming in the lower stratosphere more closely resembling LRC_{O3} (Fig. 2b) compared to HRC_{O3}. The net change results from Polvani et al. (2011) continue to show an increase in this region at the high-latitudes with cooling at the very top of the atmosphere, features that are both seen LRC_{Total} and HRC_{Total} (Fig. 2c,f). The results from the zonal mean zonal wind calculation in Polvani et al. (2011) agree with the HRC simulations shown previously (Fig.2d-f). The result of increasing concentrations is an increase and poleward shift of the westerlies that can also be seen in HRC_{CO2} (Fig. 3d). The more intense weakening and equatorward shift seen with the ozone recovery is found in HRC_{O3} (Fig. 3e). And the overall trend is an equatorward shift and weakening of the westerlies, especially in the upper 200 mb consistent with what is found in HRC_{Total} (Fig. 3f). The comparison of these results suggest that the atmospheric resolution is not as important as the ocean resolution except for the lower stratosphere in the past ozone simulation. Otherwise, the results from Polvani et al. (2011) are similar to the HRC simulations, indicating that the differences seen between the LRC and HRC experiments are due to the presence of enhanced ocean meso-scale variability.

3.3 Sea surface temperature

https://doi.org/10.5194/egusphere-2023-340
Preprint. Discussion started: 7 March 2023

Next, the results from the sea surface temperature (SST) are analyzed (Figure 4). Beginning with LRC_{CO2} (Figure 4a), there is roughly one-degree warming everywhere except in the Southern Ocean where there is intense warming observed in the Southern Ocean of nearly three-degrees. With the increase in CO_2 concentrations, there is warming everywhere in the Southern Hemisphere oceans except for one small region in the South Pacific. In the eddy-resolving case, HRC_{CO2} (Figure 4d), the results do not differ much from the eddy-parameterizing case with warming observed nearly everywhere including the Southern Ocean where the presence of eddies shows a strong increase in SSTs. This warming is seen in eddy-rich regions like the Agulhas retroflection and the Brazil-Malvinas Confluence Zone. Unlike LRC_{CO2}, however, there is cooling seen in the high-latitudes near Antarctica (see also Bilgen and Kirtman, 2020).

LRC_{O3} (Figure 4b) shows an opposite but similar pattern to LRC_{CO2} with cooling seen throughout all the oceans and warming in the same small region in the South Pacific. The HRC_{O3} simulation (Figure 4e) also shows cooling nearly everywhere except around Antarctica, where a slight warming is observed. In contrast with the low-resolution simulation, however, the cooling seen over the Southern Ocean and the ACC is much weaker. Additionally, the strong eddy response observed in HRC_{CO2} is not present with the changed ozone. As mentioned previously, the weak cooling response observed in HRC_{O3} is likely due to eddy compensation with the presence of eddies dampening the response in SSTs over the Southern Ocean as changes in atmospheric forcing are experienced (Doddridge et al., 2019).

Overall, the net change shown in LRC_{Total} (Figure 4c) is small suggesting that the increased CO_2 concentrations and 1955 ozone levels largely cancel each other out with respect to SST. In the Indian and Pacific Oceans, there is a slight warming observed, demonstrating that the CO_2 forcing is stronger here, whereas there is cooling seen everywhere else showing that the ozone signal is larger, especially near Antarctica, which with 1955 ozone levels is no longer as exposed to solar radiation. The total net change seen in HRC_{Total} (Figure 4f) is larger than LRC_{Total} mostly dominated by the ozone forcing with cooling seen in most of the Southern Hemisphere. The eddy-rich regions identified previously undergo warming and cooling highlighting the importance of both CO_2 and ozone, however, overall, the increase in CO_2 concentrations and heat trapped within the eddies plays a larger role in these regions.

3.4 Sea surface height

For the sea surface height (SSH), with an increase in CO_2 concentrations in LRC_{CO2} (Fig. 5a), there is an increase in SSH seen everywhere except south of the ACC and most of the South Atlantic. The pattern seen in HRC_{CO2} (Fig. 5d) closely resembles the pattern seen in the LRC equivalent with the exception of the eddies. In HRC_{CO2}, the magnitude of change is comparable to LRC_{CO2} and the eddies in the Agulhas retroflection and Brazil-Malvinas Confluence Zone show an increase in SSH.

For LRC_{O3} (Fig. 5b), an opposite pattern is seen compared to LRC_{CO2}, with an increase in sea level expected south of the ACC and South Atlantic with 1955 ozone levels. Once again, the pattern in the high-resolution simulation HRC_{O3} (Fig. 5e) is similar to the low-resolution simulation. The magnitude of change, however, is much smaller than what is

https://doi.org/10.5194/egusphere-2023-340
Preprint. Discussion started: 7 March 2023

seen in both LRC_{O3} and HRC_{CO2} and the eddies are not associated with much change, similar to what was shown in the HRC_{O3} SST map.

The net change is once again weak in LRC_{Total} (Fig. 5c), but the pattern resembles that of the LRC_{O3} case, especially poleward of 45°S, suggesting that the ozone forcing is slightly more important in the low-resolution eddy-parameterizing model. The SSH pattern seen in HRC_{Total} (Fig. 5f) however, closely resembles HRC_{CO2} demonstrating that the increased CO_2 concentrations dominate in the high-resolution eddy-resolving model.

3.5 Eddy kinetic energy

The eddy kinetic energy ($EKE = 0.5(u'^2 + v'^2)$, $u' = u - \bar{u}$, $v' = v - \bar{v}$) is calculated for each simulation and for LRC_{CO2} (Fig. 6a), there is a weak EKE response since it is not an eddy-resolving model. There is a small signal in the equatorial region with increases and decreases in EKE observed. In the eddy-resolving simulations, the presence of eddies is evident as the changes are seen throughout the Southern Hemisphere in HRC_{CO2} (Fig. 6d). In HRC_{CO2} (Fig. 6d) there is an increase in EKE in the ACC, the open Pacific Ocean, along the coast of Africa, through the Mozambique Channel, and the Agulhas retroflection associated with an increase in CO_2 concentrations. There is a decrease in EKE in the equatorial region, near the East Australian Current and Brazil-Malvinas Confluence Zone, and parts of the Agulhas retroflection.

LRC_{O3} (Fig. 6b) shows a similar but opposite weak response in EKE as LRC_{CO2} with the largest signal observed in the equatorial regions. Again, the high-resolution simulation HRC_{O3} (Fig. 6e), shows a larger EKE response. Compared to the HRC_{CO2} simulation, however, the HRC_{O3} simulation is less active, and values are not as large. There is an increase in EKE the equatorial Pacific and the subtropical Pacific and Indian Oceans, and a decrease seen in the majority of the ACC.

The pattern from LRC_{Total} (Fig. 6c), although small, more closely resembles the pattern from LRC_{O3}, again suggesting that the ozone forcing is slightly stronger than the increased CO_2 forcing in the eddy-parameterized model, agreeing with the result of the previous SSH figure (Fig. 5) that also shows a slightly stronger response to the 1955 ozone levels. In the high-resolution simulations, between the two forces, the increase in CO_2 is more dominant. The pattern seen in HRC_{Total} (Fig. 6f) is strikingly similar to HRC_{CO2}. The strong changes in EKE observed in response to increased CO_2 concentrations could be explained by eddy saturation, especially over the Southern Ocean where this phenomenon has been known to take place (Meredith et al., 2012; Morrison and Hogg, 2013; Marshall et al., 2017). Eddy saturation occurs when there is an intensification of the winds and an increase in the windstress (i.e., due to the increase in CO_2 concentrations) and the increased momentum is then transferred to the ocean mesoscale, therefore creating a more energetic eddy-field as a result.

3.6 Zonal mean ocean temperature

https://doi.org/10.5194/egusphere-2023-340
Preprint. Discussion started: 7 March 2023

The zonal mean ocean temperature is calculated at each latitude throughout the Southern Hemisphere (Fig. 7). With the increase in CO_2 concentrations in LRC_{CO2} (Fig. 7a), there is an increase in the ocean temperature observed throughout the entire vertical structure of the ocean with the exception of one small region of cooling found near 35°S at 1000 m. The greatest warming in this scenario is found poleward of 40°S with strong increases at the surface and 2000 m. The HRC case shows a very different response than the LRC case however, with an overall weaker, less uniform response. In HRC_{CO2} (Fig. 7d), the strongest increase in temperature is found at the surface equatorward of 50°S. In addition to the surface, there are strong increases in temperature found down to the intermediate depths near Antarctica, 50°S, and near the equator, all locations of increased EKE (Fig. 6d) with the eddies from the ACC, western boundary currents, and equatorial currents likely influencing the increase in temperature observed.

Consistent with previous results from the LRC simulations, a similar but opposite pattern is seen in LRC_{O3} (Fig. 7b) with cooling observed nearly everywhere except for the location of cooling observed in LRC_{CO2}, there is warming. In HRC_{O3} (Fig. 7e), there is cooling observed nearly everywhere with the strongest decrease in temperature found in the upper 1000 m and little change seen at deeper depths. The decrease in temperature found at 50°S is located at the same latitude where there is a strong zonal mean decrease in EKE (Fig. 6e).

The overall change in LRC_{Total} (Fig. 7c) shows that the ozone is the stronger of the two forced responses. In the LRC simulations (Fig. 7 a-c), the impact of increased CO_2 concentrations and past ozone are seen at depth suggesting a strong mixing component in the eddy-parameterizing simulations as the changes are nearly uniform throughout the water column, especially towards Antarctica. HRC_{Total} (Fig. 7f), however, shows the ozone signal is only stronger in the upper 500 m equatorward of 50°S, and that the increase in CO_2 concentrations play a larger role elsewhere, especially at the intermediate depths in eddy-rich regions. The HRC maps also show that the decrease (increase) in SST observed near Antarctica (Fig. 4a,b) with the increased CO_2 concentrations (1955 ozone levels) occurs only at the surface in the upper 200 m and there is an increase (decrease) found at the depth directly below.

3.7 Convective precipitation

The convective precipitation is analyzed (Fig. 8) rather than the total precipitation due to its stronger signal and more localized relationship with SST. The results from the eddy-parameterizing simulations are found to differ greatly from the eddy-resolving simulations. In LRC_{CO2} (Fig. 8a), there is a general increase in convective precipitation but with significant spatial heterogeneity. For example, there is an increase in convective precipitation over the equatorial regions, especially the Pacific, over all of Australia, southern South America, eastern South Africa, and over the western boundary current regions. But there is a decrease in convective precipitation found over northern and central South America and the rest of Africa. HRC_{CO2} (Fig. 8d) varies significantly from the low-resolution equivalent and shows an increase over eastern and southern Africa, tropical Indian Ocean, Pacific islands, the equatorial Pacific Ocean, and western South America. There is also a decrease seen over parts of Africa, Australia, just south of the

https://doi.org/10.5194/egusphere-2023-340
Preprint. Discussion started: 7 March 2023

equatorial Pacific, eastern South America, and the western boundary currents and their extensions as CO_2 concentrations increase.

Once again, a similar but opposite pattern is seen in LRC_{O3} (Fig. 8b) to LRC_{CO2}. The HRC_{O3} (Fig. 8e) convective precipitation pattern, however, looks much different from the LRC_{O3} simulation as was seen in the CO_2 simulation. HRC_{O3} surprisingly resembles the LRC_{CO2} simulation (Fig. 8a), however, especially with the same precipitation pattern found over the Pacific. There is a decrease in convective precipitation seen across all Southern Hemisphere land with the ozone set to 1955 levels in the high-resolution case.

The overall net change seen in LRC_{Total} (Fig. 8c) is small, however, the pattern is similar to the one seen for the past ozone forcing, with the exception of Australia, that shows a total increase in convective precipitation as in the increased CO_2 concentration simulations. On the contrary, the CO_2 forcing dominates everywhere in HRC_{Total} (Fig. 8f) except over land where the ozone forcing is stronger and leads to cooling and an associated decrease in precipitation. Additionally, HRC_{Total} differs from LRC_{Total} in that over land there is a decrease in convective precipitation found in the eddy-resolving simulation compared to an increase found in the eddy-parameterizing simulation.

3.8 Surface temperature

Lastly, the surface temperature (2 m temperature) is analyzed (Fig. 9) and the results do not differ much from the SST results seen previously (Fig. 4). In LRC_{CO2} (Fig. 9a), there is strong warming everywhere in the Southern Hemisphere, especially over the Southern Ocean. Like the SST, there is one small region of cooling found in the South Pacific and a region in South America. The high-resolution map does not differ much from the low-resolution map. HRC_{CO2} (Fig. 9d) has warming nearly everywhere other than below 60°S where there is some strong cooling over Antarctica possibly related to changes in the sea ice. This cooling at the high-latitudes corresponds to the cooling observed at the surface in the zonal mean temperature map (Fig. 2d). There is a strong increase in surface temperature over land and in the eddy-rich regions as in the LRC case.

LRC_{O3} (Fig. 9b) shows a similar and opposite pattern to LRC_{CO2} with cooling everywhere other than the tiny patches seen in the South Pacific and South America that are warming. The most intense cooling is observed over the Southern Ocean. For HRC_{O3} (Fig. 9e) there is cooling everywhere in the Southern Hemisphere excluding the area around Antarctica which shows warming. The intense cooling seen over the Southern Ocean does not exist in the eddy-resolving case as in the SST case.

The net change in LRC_{Total} (Fig. 9c) is weak once again but more closely resembles the ozone forcing aside from Africa and South America which have increasing surface temperatures and are responding to the increase in CO_2. Australia, Chile, and eastern South Africa have a cooling pattern as in the ozone case, likely because these are desert

https://doi.org/10.5194/egusphere-2023-340
Preprint. Discussion started: 7 March 2023

regions and undergo extreme cooling. Finally, the HRC_{Total} (Fig. 9f) is dominated by the ozone everywhere other than the eddy-rich regions and below 60°S that show that the increase in CO_2 concentrations is more important. Similar to the SSTs, the heat trapped within the eddies is overpowering the cooling seen from the ozone signal and showing a strong net warming change overall.

4 Conclusions

This paper, using CCSM4, investigates the role ocean model resolution plays in simulating the Southern Hemisphere climatic response to external forcing from changes in CO_2 and O_3. Ocean eddy-parameterizing (1° atmosphere and ocean) and ocean eddy-resolving (1/2° atmosphere, 1/10° ocean) simulations are analyzed to determine the importance of the ocean mesoscale processes in idealized climate experiments using past CO_2 concentrations and ozone levels. Using six experiments, LRC07/HRC07 (20^{th} century climate change forcing, constant year 2000 ozone levels), LRC08/HRC08 (constant year 2000 CO_2 and ozone levels), and LRC20/HRC20 (constant year 2000 levels and constant year 1955 ozone levels), the impact the model resolution has on the Southern Hemisphere with increased CO_2 concentrations and past ozone forcing is studied in both the atmosphere and the ocean.

Before quantitative comparisons can be made across the experiments, the initial results are normalized as the radiative forcing associated with the changes in CO_2 and O_3 are different. The results are normalized by the global mean surface air temperature with the normalized quantities interpreted as the response per degree of global mean temperature change, a method that has been used in many previous studies as discussed in the Methods section.

For both the zonal mean atmospheric temperature and zonal mean zonal wind, the difference between the eddy-parameterizing and eddy-resolving simulations shows a significant difference in the magnitude of change with more subtle differences in the spatial pattern of the response. For the zonal mean temperature, in the eddy-parameterizing simulations, the 1955 ozone forcing dominates the lower stratosphere at the high-latitudes with almost no net change seen elsewhere. In the eddy-resolving simulations, however, the ozone forcing is strong throughout the Southern Hemisphere whereas both the CO_2 and ozone concentrations affect the lower stratosphere at the high-latitudes. In the low-resolution eddy-parameterizing simulation, the increased CO_2 and 1955 ozone levels are nearly equal and opposite for the zonal mean zonal wind with no shift of the westerlies observed. In the high-resolution eddy-resolving experiment, the increased CO_2 concentrations dominate equatorward of 40°S and the ozone forcing poleward of 40°S with the westerly jet shifting equatorward overall. For the sea surface temperatures in the eddy-parameterized simulations, the increase in CO_2 concentrations and 1955 ozone levels are found to be nearly equal but opposite of each other with a small overall change observed. In the case of the eddy-resolving simulations, the ozone forcing (cooling) dominates throughout the Southern Hemisphere apart from eddy-rich regions like the ACC, where the increase in CO_2 response is stronger (warming). In the Southern Ocean near Antarctica, however, there is an overall weaker response in the sea surface temperatures, likely a result of eddy compensation as the mesoscale eddies prevent the wind-driven upwelling in the region. In the eddy-parameterizing simulations, the ozone plays a slightly larger role

https://doi.org/10.5194/egusphere-2023-340
Preprint. Discussion started: 7 March 2023

for the sea surface height, eddy kinetic energy, zonal mean ocean temperature, and convective precipitation. For the eddy-resolving simulations, however, the increase in CO_2 concentrations dominates with the HRC_{Total} spatial maps closely resembling the increased CO_2 concentration experiment (HRC_{CO2}). For the surface temperature in the eddy-parameterizing simulations, the increase in CO_2 concentration response (warming) is stronger over Africa and South America, but over Australia and the Southern Ocean, the 1955 ozone forcing is more important (cooling). In the eddy-resolving simulation, the ozone is stronger everywhere (cooling), including over land, except in eddy-rich regions and the Southern Ocean near Antarctica. The response of the surface temperature over Australia is unique in that Australia is seen to be cooling in response to the 1955 ozone levels in both the eddy-parameterizing and eddy-resolving simulations, despite Africa and South America warming as a result of the increased CO_2 concentrations in the eddy-parameterizing simulations. These results show that the model resolution (eddy-parameterizing versus eddy-resolving) proves to be important in how the Southern Hemisphere responds to changes in external forcing (increased CO_2 concentrations versus 1955 ozone levels).

There are a few caveats to note with the conclusion of this study. The first is that this is an idealized study and the results presented are not to be interpreted as projections or predictions of future climate, but rather this is an investigation of how extreme changes in the external forcing can lead to different responses in the eddy-parameterizing and eddy-resolving simulations. The second caveat regards the difference in atmospheric resolution between the eddy-parameterizing (1°) and eddy-resolving (1/2°) simulations. Because the atmospheric resolution is not consistent between the two, it is possible that some of the changes observed could be due to the difference in atmospheric resolution and not the ocean resolution, especially in the lower stratosphere where the ozone is depleting. The comparison with Polvani et al. (2011) gives some confidence that the ocean resolution is more important, however, a study that keeps the same atmospheric resolution across all the experiments may improve the results. Lastly, while it has been shown that the ozone forcing is strongly seasonal with its largest impact observed in austral summer (DJF), all months are considered in the time averaged mean in this study. This is done for both the 20th century CO_2 and 1955 O_3 levels experiments so the results are consistent with each other.

The differences observed in the Southern Hemisphere in response to changes in model resolution is significant and emphasizes the need for an increase in model resolution going forward, especially in climate prediction studies. Global coupled-climate models in the past are eddy-parameterizing and this study shows that the results may vary considerably if the models were eddy-resolving. This will be increasingly important as CO_2 concentrations continue to increase and there is a need for more accurate climate forecasts, especially in instances where the associated warming from the CO_2 forced signal overcomes the cooling response associated with the O_3.

https://doi.org/10.5194/egusphere-2023-340
Preprint. Discussion started: 7 March 2023

Code and data availability. The CCSM4 user guide, description, and code can be downloaded at https://www2.cesm.ucar.edu/models/ccsm4.0/ccsm/. The CCSM4 data used in this study is on the University of Miami's Rosenstiel School of Marine, Atmospheric, and Earth Science's computer clusters, Eddy and Mango.

Author contributions. Houraa Daher and Ben P. Kirtman contributed to the study conception and design. Model simulations were run by both authors. Material preparation, data collection and analysis were performed by Houraa Daher. The first draft of the manuscript was written by Houraa Daher and both authors commented on previous versions of the manuscript. Both authors read and approved the final manuscript.

Competing interests. The contact author has declared that none of the authors have competing interests.

Acknowledgements. The authors acknowledge the support from the National Oceanic and Atmospheric Administration (NA18OAR4310293, NA15OAR4320064), the National Science Foundation (OCE1419569, OCE1559151), and the Department of Energy (DE-SC0019433).

https://doi.org/10.5194/egusphere-2023-340
Preprint. Discussion started: 7 March 2023

References

Bilgen, S. I., and Kirtman, B. P.: Impact of ocean model resolution on understanding the delayed warming of the Southern Ocean. Environ. Res. Lett., 15(11), 114012, 2020

Bitz, C. M., and Polvani, L. M.: Antarctic climate response to stratospheric ozone depletion in a fine resolution ocean climate model. Geophys. Res. Lett., 39(20), 2012

Bryan, F. O., Tomas, R., Dennis, J. M., Chelton, D. B., Loeb, N. G., and McClean, J. L.: Frontal scale air–sea interaction in high-resolution coupled climate models. J. Clim., 23(23), 6277-6291, 2010

Chang, P., Zhang, S., Danabasoglu, G., Yeager, S. G., Fu, H., Wang, H., Castruccio, F.S., Chen, Y., Edwards, J., Fu, D. and Jia, Y.: An unprecedented set of high-resolution earth system simulations for understanding multiscale interactions in climate variability and change. J. Adv. Model. Earth Syst., 12(12), e2020MS002298, 2020

Cheng, Y., Putrasahan, D., Beal, L., and Kirtman, B.: Quantifying Agulhas leakage in a high-resolution climate model. J. Clim., 29(19), 6881-6892, 2016

Doddridge, E. W., Marshall, J., Song, H., Campin, J. M., Kelley, M., and Nazarenko, L.: Eddy compensation dampens Southern Ocean sea surface temperature response to westerly wind trends. Geophys. Res. Lett., 46(8), 4365-4377, 2019

Eyring, V., Arblaster, J. M., Cionni, I., Sedláček, J., Perlwitz, J., Young, P. J., Bekki, S., Bergmann, D., Cameron-Smith, P., Collins, W.J., and Faluvegi, G.: Long-term ozone changes and associated climate impacts in CMIP5 simulations. J. Geophys. Res. Atmos., 118(10), 5029-5060, 2013

Gent, P. R., Danabasoglu, G., Donner, L. J., Holland, M. M., Hunke, E. C., Jayne, S. R., Lawrence, D.M., Neale, R. B., Rasch, P. J., Vertenstein, M., and Worley, P.H..: The community climate system model version 4. J. Clim., 24(19), 4973-4991., 2011

Gnanadesikan, A., Pradal, M. A., and Abernathey, R.: Isopycnal mixing by mesoscale eddies significantly impacts oceanic anthropogenic carbon uptake. Geophys. Res. Lett., 42(11), 4249-4255, 2015

Goyal, R., Sen Gupta, A., Jucker, M., and England, M. H.: Historical and projected changes in the Southern Hemisphere surface westerlies. Geophys. Res. Lett., 48(4), e2020GL090849, 2021

Hahn, L. C., Armour, K. C., Zelinka, M. D., Bitz, C. M., and Donohoe, A.: Contributions to polar amplification in CMIP5 and CMIP6 models. Front. Earth Sci., 9, 710036, 2021

https://doi.org/10.5194/egusphere-2023-340
Preprint. Discussion started: 7 March 2023

Hewitt, H. T., Roberts, M. J., Hyder, P., Graham, T., Rae, J., Belcher, S. E., Bourdallé-Badie, R., Copsey, D., Coward, A., Guiavarch, C., and Harris, C.: The impact of resolving the Rossby radius at mid-latitudes in the ocean: Results from a high-resolution version of the Met Office GC2 coupled model. Geosci. Model Dev., 9(10), 3655-3670, 2016

Holland, M. M., and Bitz, C. M.: Polar amplification of climate change in coupled models. Clim. Dyn., 21(3-4), 221-232, 2003

Ivanciu, I., Matthes, K., Biastoch, A., Wahl, S., and Harlaß, J.: Twenty-first-century Southern Hemisphere impacts of ozone recovery and climate change from the stratosphere to the ocean. Weather Clim. Dynam., 3(1), 139-171., 2022

Kelly, K. A., Small, R. J., Samelson, R. M., Qiu, B., Joyce, T. M., Kwon, Y. O., and Cronin, M. F.: Western boundary currents and frontal air–sea interaction: Gulf Stream and Kuroshio Extension. J. Clim., 23(21), 5644-5667, 2010

Kirtman, B. P., Bitz, C., Bryan, F., Collins, W., Dennis, J., Hearn, N., Kinter, J. L., Loft, R., Rousset, C., Siqueira, L., and Stan, C.: Impact of ocean model resolution on CCSM climate simulations. Clim. Dyn., 39, 1303-1328, 2012

Lamarque, J. F., Bond, T. C., Eyring, V., Granier, C., Heil, A., Klimont, Z., Lee, D., Liousse, C., Mieville, A., Owen, B., and Schultz, M.G.: Historical (1850–2000) gridded anthropogenic and biomass burning emissions of reactive gases and aerosols: methodology and application. Atmospheric Chem. Phys., 10(15), 7017-7039, 2010

Lamarque, J. F., Kyle, G. P., Meinshausen, M., Riahi, K., Smith, S. J., van Vuuren, D. P., Conley, A. J., and Vitt, F.: Global and regional evolution of short-lived radiatively-active gases and aerosols in the Representative Concentration Pathways. Clim. Change, 109, 191-212, 2011

Lamarque, J. F., Emmons, L. K., Hess, P. G., Kinnison, D. E., Tilmes, S., Vitt, F., Heald, C., Holland, E.A., Lauritzen, P., Neu, J., and Orlando, J.J.: CAM-chem: Description and evaluation of interactive atmospheric chemistry in the Community Earth System Model. Geosci. Model Dev., 5(2), 369-411, 2012

Lin, L., Gettelman, A., Fu, Q., and Xu, Y.: Simulated differences in 21st century aridity due to different scenarios of greenhouse gases and aerosols. Clim. Change, 146, 407-422, 2018

Ma, X., Jing, Z., Chang, P., Liu, X., Montuoro, R., Small, R. J., Bryan, F. O., Greatbatch, R. J., Brandt, P., Wu, D. and Lin, X.: Western boundary currents regulated by interaction between ocean eddies and the atmosphere. Nature, 535(7613), 533-537, 2016

https://doi.org/10.5194/egusphere-2023-340
Preprint. Discussion started: 7 March 2023

Marshall, D. P., Ambaum, M. H., Maddison, J. R., Munday, D. R., and Novak, L.: Eddy saturation and frictional control of the Antarctic Circumpolar Current. Geophys. Res. Lett., 44(1), 286-292, 2017

McClean, J. L., Bader, D. C., Bryan, F. O., Maltrud, M. E., Dennis, J. M., Mirin, A. A., Jones, P. W., Kim, Y. Y., Ivanova, D. P., Vertenstein, M., and Boyle, J.S.: A prototype two-decade fully-coupled fine-resolution CCSM simulation. Ocean Model., 39(1-2), 10-30., 2011

Meehl, G. A., Washington, W. M., Arblaster, J. M., Hu, A., Teng, H., Tebaldi, C., Sanderson, B. N., Lamarque, J. F, Conley, A., Strand, W.G. and White, J.B.: Climate system response to external forcings and climate change projections in CCSM4. J. Clim., 25(11), 3661-3683, 2012

Meredith, M. P., Naveira Garabato, A. C., Hogg, A. M., and Farneti, R.: Sensitivity of the overturning circulation in the Southern Ocean to decadal changes in wind forcing. J. Clim., 25(1), 99-110, 2012

Morrison, A. K., and Hogg, A. M.: On the relationship between Southern Ocean overturning and ACC transport. J Phys Oceanogr., 43(1), 140-148., 2013

Oliver, E. C. J., and Holbrook, N. J.: Extending our understanding of South Pacific gyre "spin-up": Modeling the East Australian Current in a future climate. J. Geophys. Res. Oceans, 119(5), 2788-2805, 2014

Polvani, L. M., Previdi, M., and Deser, C.: Large cancellation, due to ozone recovery, of future Southern Hemisphere atmospheric circulation trends. Geophys. Res. Lett., 38(4), 2011

Putrasahan, D. A., Miller, A. J., and Seo, H.: Isolating mesoscale coupled ocean–atmosphere interactions in the Kuroshio Extension region. Dyn. Atmospheres Oceans, 63, 60-78, 2013

Putrasahan, D. A., Beal, L. M., Kirtman, B. P., and Cheng, Y.: A new Eulerian method to estimate "spicy" Agulhas leakage in climate models. Geophys. Res. Lett., 42(11), 4532-4539, 2015

Putrasahan, D. A., Kamenkovich, I., Le Hénaff, M., and Kirtman, B. P.: Importance of ocean mesoscale variability for air-sea interactions in the Gulf of Mexico. Geophys. Res. Lett., 44(12), 6352-6362., 2017

Rantanen, M., Karpechko, A. Y., Lipponen, A., Nordling, K., Hyvärinen, O., Ruosteenoja, K., Vihma, T., and Laaksonen, A.: The Arctic has warmed nearly four times faster than the globe since 1979. Commun. Earth Environ., 3(1), 168., 2022

https://doi.org/10.5194/egusphere-2023-340
Preprint. Discussion started: 7 March 2023

Sallée, J. B., Matear, R. J., Rintoul, S. R., and Lenton, A.: Localized subduction of anthropogenic carbon dioxide in the Southern Hemisphere oceans. Nat. Geosci., 5(8), 579-584, 2012

Small, R. D., deSzoeke, S. P., Xie, S. P., O'neill, L., Seo, H., Song, Q., Cornillon, P., Spall, M., and Minobe, S.: Air–sea interaction over ocean fronts and eddies. Dyn. Atmospheres Oceans, 45(3-4), 274-319, 2008

Small, R. J., Msadek, R., Kwon, Y. O., Booth, J. F., and Zarzycki, C.: Atmosphere surface storm track response to resolved ocean mesoscale in two sets of global climate model experiments. Clim. Dyn., 52, 2067-2089, 2019

Small, R. J., Bryan, F. O., Bishop, S. P., Larson, S., and Tomas, R. A.: What drives upper-ocean temperature variability in coupled climate models and observations?. J. Clim., 33(2), 577-596, 2020

Soden, B. J., and Vecchi, G. A.: The vertical distribution of cloud feedback in coupled ocean-atmosphere models. Geophys. Res. Lett., 38(12)., 2011

Swart, S., Gille, S. T., Delille, B., Josey, S., Mazloff, M., Newman, L., Thompson, A.F., Thomson, J., Ward, B., Du Plessis, M.D. and Kent, E.C.: Constraining Southern Ocean air-sea-ice fluxes through enhanced observations. Front. Mar. Sci., 6, 421., 2019

Vecchi, G. A., and Soden, B. J.: Global warming and the weakening of the tropical circulation. J. Clim., 20(17), 4316-4340, 2007

Wu, L., Cai, W., Zhang, L., Nakamura, H., Timmermann, A., Joyce, T., McPhaden, M.J., Alexander, M., Qiu, B., Visbeck, M. and Chang, P.: Enhanced warming over the global subtropical western boundary currents. Nat. Clim. Change., 2(3), 161-166., 2012

Zhao, C., Liu, B., Piao, S., Wang, X., Lobell, D. B., Huang, Y., Huang, M., Yao, Y., Bassu, S., Ciais, P. and Durand, J.L.: Temperature increase reduces global yields of major crops in four independent estimates. Proc. Natl. Acad. Sci., 114(35), 9326-9331, 2017

https://doi.org/10.5194/egusphere-2023-340
Preprint. Discussion started: 7 March 2023

Tables

Table 1. List of the six CCSM4 experiments used in this study. Low-resolution is equal to 1° in both the atmosphere and ocean, high-resolution is 1/2° in the atmosphere and 1/10° in the ocean.

Name	Resolution	CO_2 concentrations	Ozone	Years
LRC07	Low	Historical CO_2	Year 2000 O_3	100 years
LRC08	Low	Year 2000 CO_2	Year 2000 O_3	100 years
LRC20	Low	Year 2000 CO_2	Year 1955 O_3	100 years
HRC07	High	Historical CO_2	Year 2000 O_3	70 years
HRC08	High	Year 2000 CO_2	Year 2000 O_3	70 years
HRC20	High	Year 2000 CO_2	Year 1955 O_3	20 years

https://doi.org/10.5194/egusphere-2023-340
Preprint. Discussion started: 7 March 2023

580 **Figures**

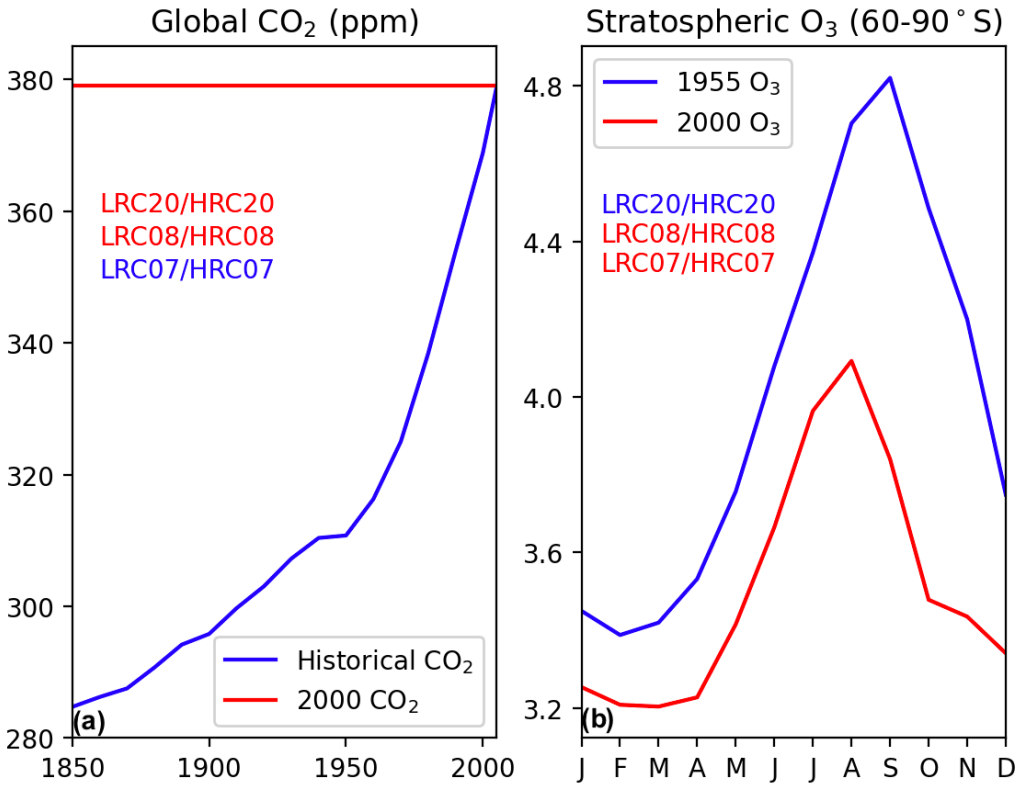

Figure 1. The CO_2 concentrations and O_3 forcing used in the CCSM4 simulations. **(a)** The year 2000 CO_2 levels shown in red (LRC08/HRC08 and LRC20/HRC20) and historical ozone shown in blue (LRC07/HRC07). **(b)** The 1955 ozone levels shown in blue (LRC20/HRC20) and the 2000 ozone levels shown in red (LRC07/HRC07 and LRC08/HRC08).

https://doi.org/10.5194/egusphere-2023-340
Preprint. Discussion started: 7 March 2023

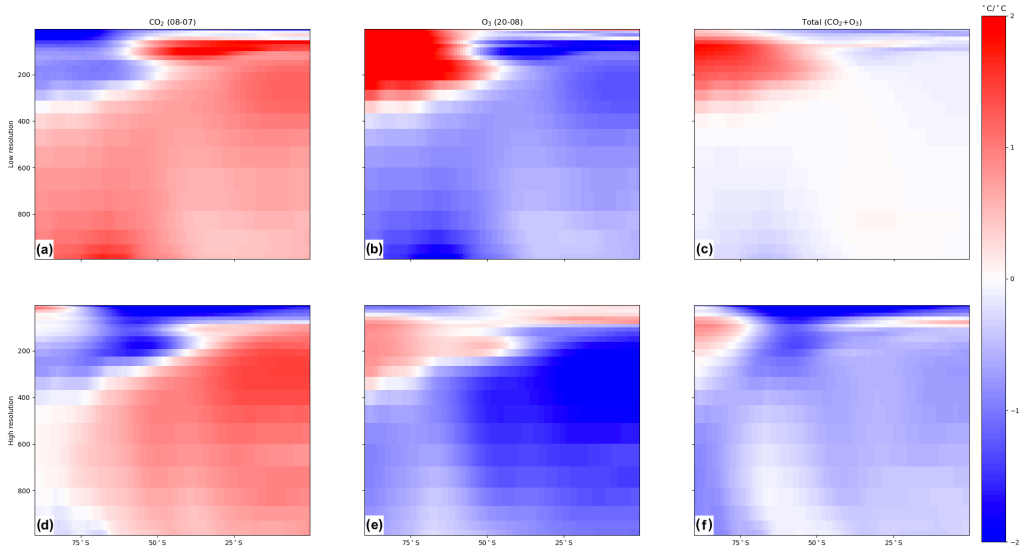

585

Figure 2. The zonal mean Southern Hemisphere atmospheric temperature in the eddy-parameterizing simulations **(a-c)** and eddy-resolving simulations **(d-f)** for the increased CO_2 concentrations **(a and d)**, past ozone from 1955 **(b and e)**, and net change **(c and f)**.

https://doi.org/10.5194/egusphere-2023-340
Preprint. Discussion started: 7 March 2023

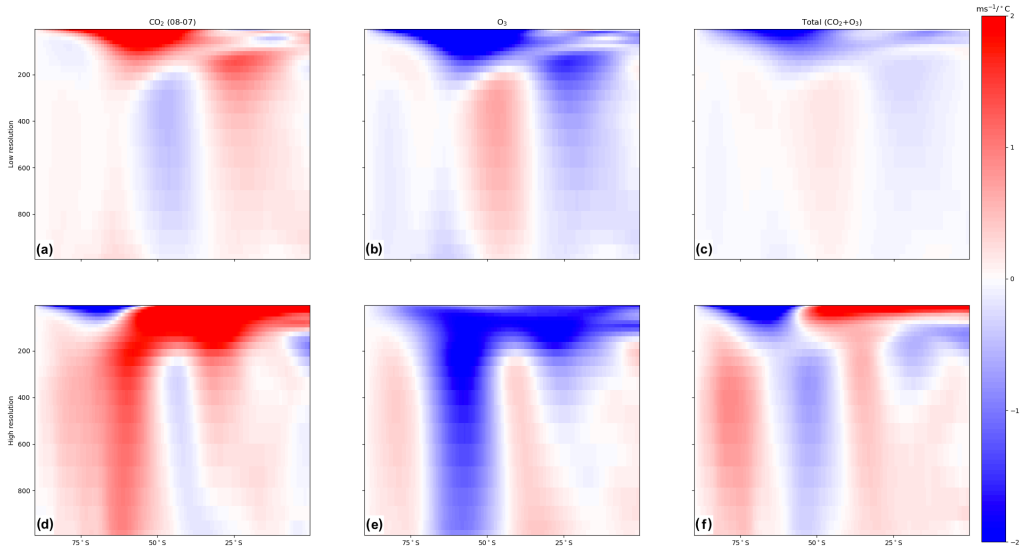

590 **Figure 3.** Same as in Figure 2 but for zonal mean zonal wind.

https://doi.org/10.5194/egusphere-2023-340
Preprint. Discussion started: 7 March 2023

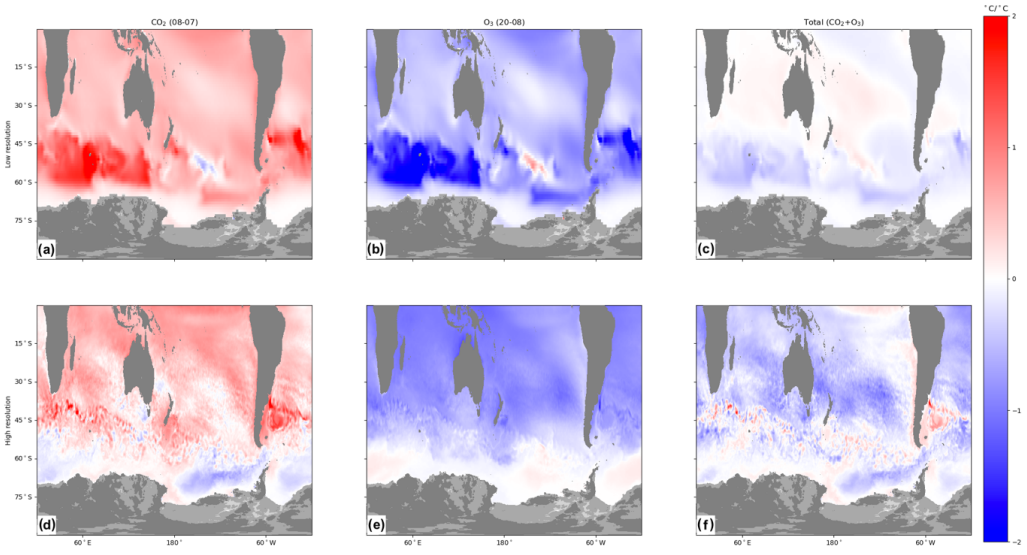

Figure 4. Same as in Figure 2 but for sea surface temperature.

https://doi.org/10.5194/egusphere-2023-340
Preprint. Discussion started: 7 March 2023

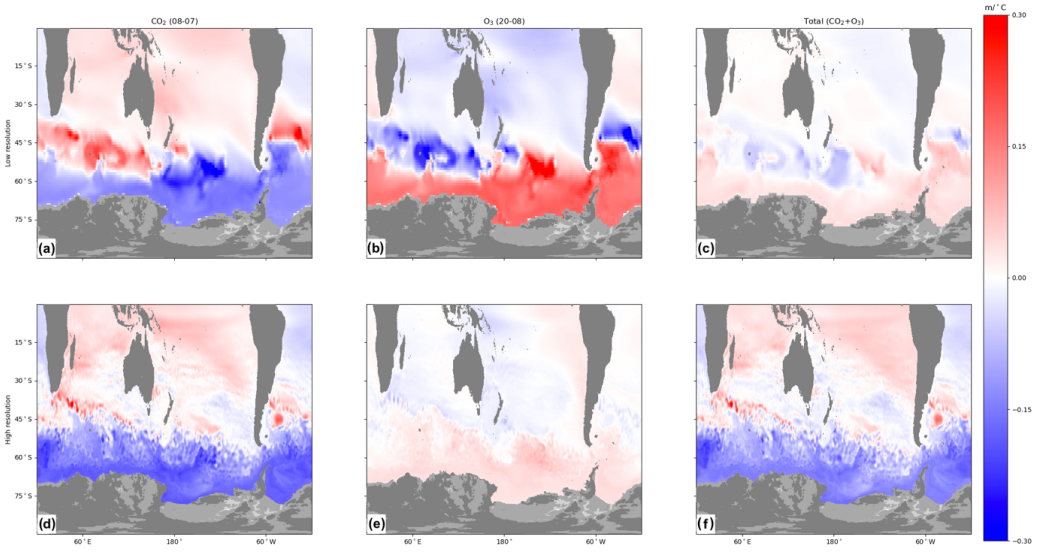

595 **Figure 5.** Same as in Figure 2 but for sea surface height.

https://doi.org/10.5194/egusphere-2023-340
Preprint. Discussion started: 7 March 2023

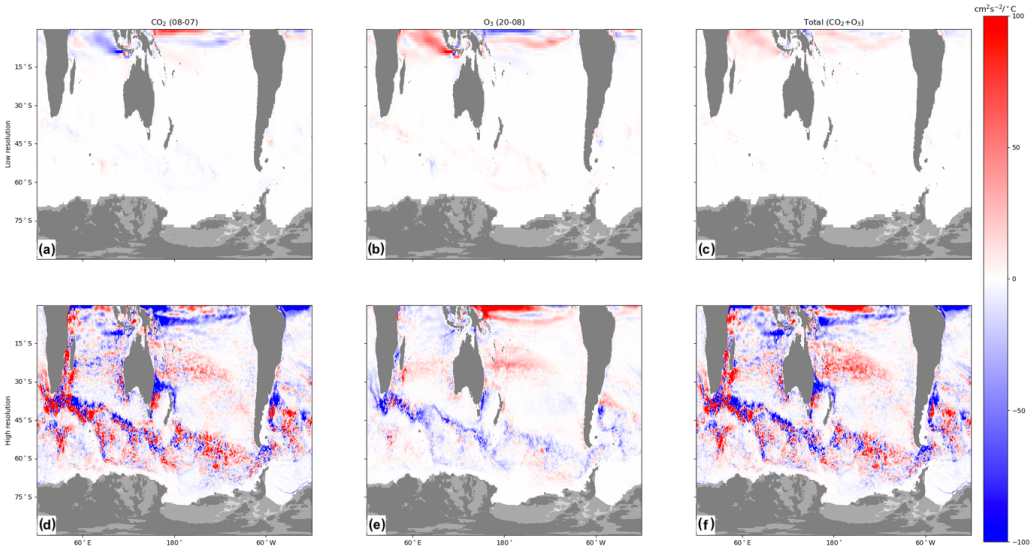

Figure 6. Same as in Figure 2 but for eddy kinetic energy.

https://doi.org/10.5194/egusphere-2023-340
Preprint. Discussion started: 7 March 2023

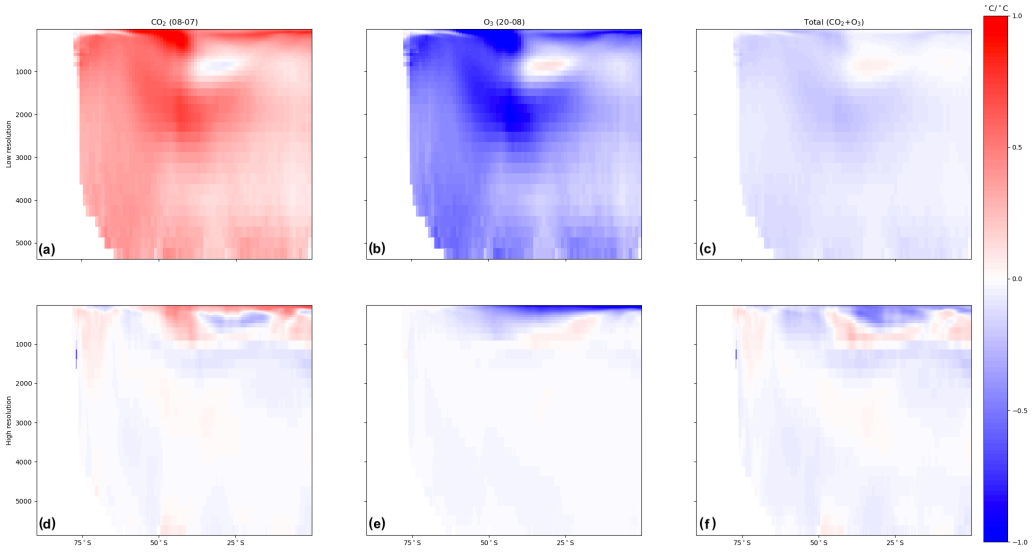

Figure 7. Same as in Figure 2 but for zonal mean ocean temperature.

https://doi.org/10.5194/egusphere-2023-340
Preprint. Discussion started: 7 March 2023

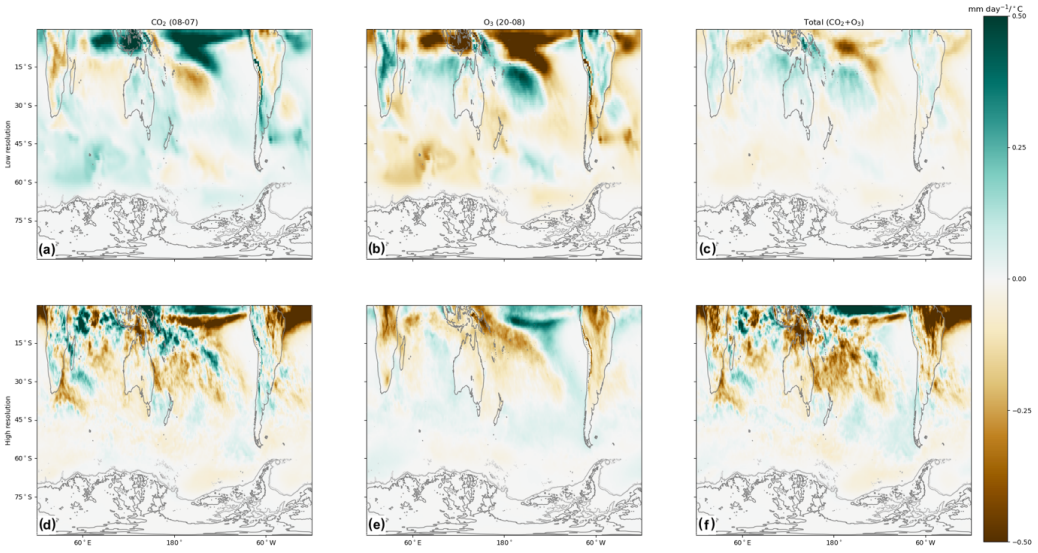

600

Figure 8. Same as in Figure 2 but for convective precipitation.

https://doi.org/10.5194/egusphere-2023-340
Preprint. Discussion started: 7 March 2023

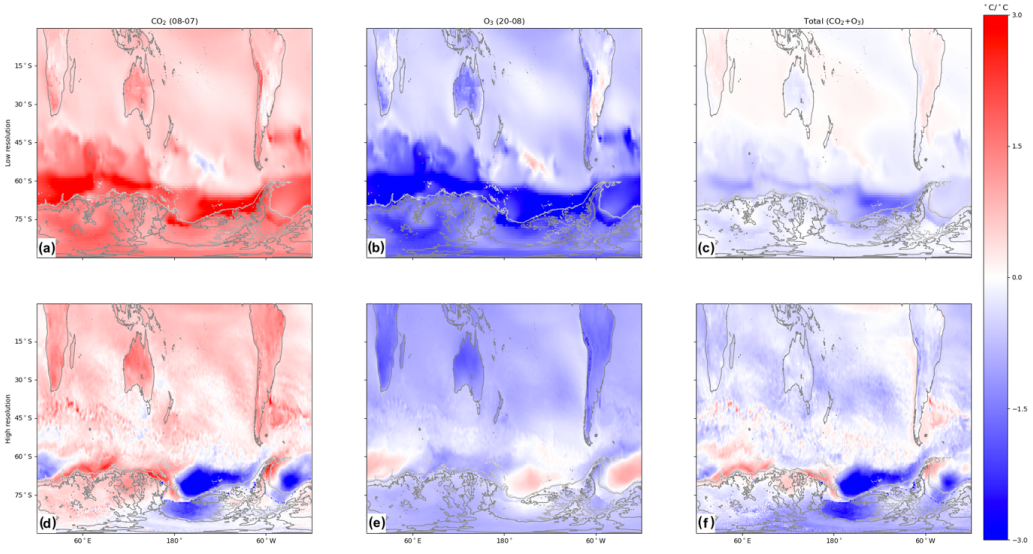

Figure 9. Same as in Figure 2 but for surface temperature (2 m temperature).